



Electro-optic and dielectric properties of Zirconium-doped congruent lithium-niobate crystals

Mustapha Abarkan, Michel Aillerie, Ninel Kokanyan, Clément Teyssandier,
Edvard Kokanyan

► To cite this version:

Mustapha Abarkan, Michel Aillerie, Ninel Kokanyan, Clément Teyssandier, Edvard Kokanyan. Electro-optic and dielectric properties of Zirconium-doped congruent lithium-niobate crystals. Optical Materials Express, 2014, 4 (1), pp.179-189. 10.1364/OME.4.000179 . hal-01467230

HAL Id: hal-01467230

<https://hal.science/hal-01467230>

Submitted on 14 Feb 2017

HAL is a multi-disciplinary open access archive for the deposit and dissemination of scientific research documents, whether they are published or not. The documents may come from teaching and research institutions in France or abroad, or from public or private research centers.

L'archive ouverte pluridisciplinaire **HAL**, est destinée au dépôt et à la diffusion de documents scientifiques de niveau recherche, publiés ou non, émanant des établissements d'enseignement et de recherche français ou étrangers, des laboratoires publics ou privés.

Electro-optic and dielectric properties of Zirconium-doped congruent lithium–niobate crystals

Mustapha Abarkan,^{1,2,3} Michel Aillerie,^{2,3,*} Ninel Kokanyan,^{2,3} Clément Teyssandier,^{2,3} and Edvard Kokanyan^{4,5}

¹Université Sidi Mohammed Ben Abdellah de Fès, Faculté Polydisciplinaire de Taza, Laboratoire LIMAO, BP 1223 Taza-Gare, Morocco

²Université de Lorraine, LMOPS, EA-4423, 2 rue E. Belin, 57070 Metz, France

³Supelec, LMOPS, 2 rue E. Belin, 57070 Metz, France

⁴Institute for Physical Research, National Academy of Sciences of Armenia, 0203, Ashtarak, Armenia

⁵Armenian State Pedagogical University After Kh. Abovyan, Tigran Metsi Ave., 17, Yerevan, Armenia
aillerie@metz.supelec.fr

Abstract: Measurements of electro-optic and dielectric properties in Zirconium (Zr)-doped lithium niobate (LN:Zr) crystals are performed as functions of the dopant concentration in the range 0.0–2.5 mol%. The clamped and unclamped electro-optic coefficients r_{22} of Zr-doped LN and the corresponding dielectric permittivity as well, have been experimentally determined and compared with the results obtained in undoped congruent LN crystals. We show that the electro-optic and dielectric properties present a kink around 2 mol% of zirconium which seems to be the “threshold” concentration required to strongly reduce the photorefractive effect. All reported results confirm that the LN:Zr is a very promising candidate for several non linear devices.

©2014 Optical Society of America

OCIS codes: (160.2100) Electro-optical materials; (160.3730) Lithium niobate; (120.5060) Phase modulation; (120.3180) Interferometry.

References and links

1. J. F. McCannt, J. Pezytg, and P. Wilsen, “A versatile electronic light shutter composed of a high speed switching circuit coupled with a lithium niobate Pockels cell,” *J. Phys. E Sci. Instrum.* **15**, 322–324 (1982).
2. S. Zhang, Q. Wang, X. Xu, C. Dong, X. Zhang, and P. Li, “Diode-laser pumped passively Q-switched green laser by intracavity frequency-doubling with periodically poled LiNbO₃,” *Opt. Laser Technol.* **35**(3), 233–235 (2003).
3. E. Krätzig and O. F. Schirmer, “Photorefractive centers in electro-optic crystals,” in *Photorefractive Materials and their Applications I*, P. Günter and J. P. Huignard, eds. (Springer, 1988), pp. 131–167.
4. G. P. Banfi, P. K. Datta, V. Degiorgio, and D. Fortusini, “Wavelength shifting and amplification of optical pulses through cascaded second-order processes in periodically poled lithium niobate,” *Appl. Phys. Lett.* **73**, 136–138 (1998).
5. T. Volk and M. Wöhlecke, in *Lithium Niobate: Defects, Photorefraction and Ferroelectric Switching* (Springer-Verlag, 2008).
6. D. Eimerl, S. Velsko, L. Davis, and F. Wang, “Progress in nonlinear optical materials for high power lasers,” *Prog. Cryst. Growth Charact. Mater.* **20**(1–2), 59–113 (1990).
7. K. Polgár, L. Kovács, I. Földvári, and I. Cravero, “Spectroscopic and electrical conductivity investigation of Mg doped LiNbO₃ single crystals,” *Solid State Commun.* **59**(6), 375–379 (1986).
8. G. Zhong, J. Jin, and Z. Wu, in *Proceedings of the 11th International Quantum Electronics Conference IQEC '80*, (IEEE, 1980), p. 631.
9. T. R. Volk, N. M. Rubinina, and M. Wöhlecke, “Optical-damage-resistant impurities in lithium niobate,” *J. Opt. Soc. Am. B* **11**, 1681–1687 (1994).
10. Y. Furukawa, M. Sato, K. Kitamura, Y. Yajima, and M. Minakata, “Optical damage resistance and crystal quality of LiNbO₃ single crystals with various [Li]/[Nb] ratios,” *J. Appl. Phys.* **72**(8), 3250 (1992).
11. D. A. Bryan, R. Gerson, and H. E. Tomaschke, “Increased optical damage resistance in lithium niobate,” *Appl. Phys. Lett.* **44**(9), 847–849 (1984).
12. T. Volk, V. Pryalkin, and N. Rubinina, “Optical-damage-resistant LiNbO₃:Zn crystal,” *Opt. Lett.* **15**, 996–998 (1990).
13. E. P. Kokanyan, L. Razzari, I. Cristiani, V. Degiorgio, and J. B. Gruber, “Reduced photorefraction in hafnium-doped single-domain and periodically poled lithium niobate crystals,” *Appl. Phys. Lett.* **84**, 1880–1882 (2004).

14. L. Razzari, P. Minzioni, I. Cristiani, V. Degiorgio, and E. P. Kokanyan, "Photorefractivity of Hafnium-doped congruent lithium-niobate crystals," *Appl. Phys. Lett.* **86**, 131914 (2005).
15. S. Li, S. Liu, Y. Kong, D. Deng, G. Gao, Y. Li, H. Gao, L. Zhang, Z. Hang, S. Chen, and J. Xu, "The optical damage resistance and absorption spectra of $\text{LiNbO}_3\text{:Hf}$ crystals," *J. Phys. Condens. Matter* **18**, 3527–3534 (2006).
16. M. Abarkan, M. Aillerie, J. P. Salvestrini, M. D. Fontana, and E. P. Kokanyan, "Electro-optic and dielectric properties of Hafnium-doped congruent lithium niobate crystals," *Appl. Phys. B* **92**, 603–608 (2008).
17. P. Minzioni, I. Cristiani, V. Degiorgio, and E. P. Kokanyan, "Strongly sublinear growth of the photorefractive effect for increasing pump intensities in doped lithium-niobate crystals," *J. Appl. Phys.* **101**, 116105 (2007).
18. P. Minzioni, I. Cristiani, J. Yu, J. Parravicini, E. P. Kokanyan, and V. Degiorgio, "Linear and nonlinear optical properties of Hafnium-doped lithium-niobate crystals," *Opt. Express* **15**, 14171 (2007).
19. E. P. Kokanyan, "Hafnium-doped periodically poled lithium niobate crystals: Growth and photorefractive properties," *Ferroelectrics* **341**, 119–124 (2006).
20. A. M. Petrosyan, R. K. Hovsepyan, E. P. Kokanyan, and R. S. Feigelson, "Growth and evaluation of lithium niobate crystals containing nonphotorefractive dopants," *Proc. SPIE* **4060**, 106–113 (2000).
21. Y. Kong, S. Liu, Y. Zhao, H. Liu, S. Chen, and J. Xu, "Highly optical damage resistant crystal: Zirconium-oxide-doped lithium niobate," *Appl. Phys. Lett.* **91**(8), 081908 (2007).
22. H. Liu, Q. Liang, M. Zhu, W. Li, S. Liu, L. Zhang, S. Chen, Y. Kong, and J. Xu, "An excellent crystal for high resistance against optical damage in visible-UV range: near-stoichiometric zirconium-doped lithium niobate," *Opt. Express* **19**(3), 1734–1748 (2011).
23. N. Argiolas, M. Bazzan, M. V. Ciampolillo, P. Pozzobon, C. Sada, L. Saoner, A. M. Zaltron, L. Bacci, P. Minzioni, G. Nava, J. Parravicini, W. Yan, I. Cristiani, and V. Degiorgio, "Structural and optical properties of zirconium doped lithium niobate crystals," *J. Appl. Phys.* **108**(9), 093508 (2010).
24. L. Kovacs, G. Ruschhaupt, K. Polgar, G. Corradi, and M. Wohlecke, "Composition dependence of the ultraviolet absorption edge in lithium niobate," *Appl. Phys. Lett.* **70**(21), 2801–2803 (1997).
25. M. Aillerie, N. Theofanous, and M. D. Fontana, "Measurement of the electro-optic coefficients: description and comparison of the experimental techniques," *Invited Review Paper Appl. Phys. B* **70**, 317–334 (2000).
26. M. Abarkan, J. P. Salvestrini, M. Aillerie, and M. D. Fontana, "Frequency and wavelength dependences of electro-optic coefficients in inorganic crystals," *Appl. Opt.* **42**, 2346–2353 (2003).
27. G. Nava, P. Minzioni, W. Yan, J. Parravicini, D. Grando, E. Musso, I. Cristiani, N. Argiolas, M. Bazzan, M. V. Ciampolillo, A. Zaltron, C. Sada, and V. Degiorgio, "Zirconium-doped lithium niobate: photorefractive and electro-optical properties as a function of dopant concentration," *Opt. Mater. Express* **1**(2), 270–277 (2011).
28. F. Abdi, M. Aillerie, M. Fontana, P. Bourson, T. Volk, B. Maximov, S. Sulyanov, N. Rubinia, and M. Wohlecke, "Influence of Zn doping on electrooptical properties and structure parameters of lithium niobate crystals," *Appl. Phys. B* **68**, 795 (1999).
29. B. C. Grabmaier and F. Otto, "Growth and investigation in MgO-doped LiNbO_3 ," *J. Cryst. Growth* **79**, 682 (1986).
30. J. Salvestrini, M. D. Fontana, B. Wyncke, and F. Brehat, "Comparative measurements of the frequency dependence of the electrooptical and dielectric coefficient in inorganic crystals," *Nonlinear Optics* **17**, 271 (1997).
31. I. P. Kaminow, *An Introduction to Electro-Optic Devices* (Academic Press, 1974).
32. J. F. Nye, *Physical Properties of Crystals* (Oxford Univ. Press, 1957).
33. M. Jazbinsek and M. Zgonik, "Material tensor parameters of LiNbO_3 relevant for electro- and elasto-optics," *Appl. Phys. B* **74**, 407–414 (2002).
34. A. W. Warner, M. Onoe, and G. A. Coquin, "Determination of elastic and piezoelectric constants for crystals in class (3m)," *J. Acoust. Soc. Am.* **46**(6), 1223–1231 (1966).
35. R. W. Dixon and M. G. Cohen, "A new technique for measuring magnitudes of photoelastic tensors and its application to lithium niobate," *Appl. Phys. Lett.* **8**, 205–207 (1966).
36. A. Yariv and P. Yeh, *Optical Waves in Crystals*, (John Wiley, 1984).
37. J. P. Salvestrini, M. Abarkan, and M. D. Fontana, "Comparative study of nonlinear optical crystals for electro-optic Q-switching of laser resonators," *Opt. Mater.* **26**, 449 (2004).

1. Introduction

Lithium niobate, LiNbO_3 (LN) crystals are studied extensively and used in many applications thanks to their large piezoelectric, electro-optic and nonlinear coefficients. LN offers good transmission and high extinction ratio with a modest driving voltage in the transverse configuration, i.e. when an electric field is applied perpendicular to the direction of the optical beam. Thus, LN has a wide range of applications in electro-optic (EO) modulation and laser Q-switching [1–4]. Nevertheless, the performances of Q-switched devices require EO materials with a relatively low driving voltage and especially a high resistance to optical damage. The EO properties of LN, and particularly the coefficient r_{222} , are acceptable, but the optical damage threshold in crystals with the congruent composition is very low (0.3 GW/cm^2) compared with other optical materials [5, 6]. This is mainly the reason why the use of pure LN congruent crystals on applications requiring high power laser pulses is limited.

The main optical damage process in LN crystals is the photorefractive damage originates from the photo-generation by the optical beam of mobile charge carriers in the bright region that migrate toward the dark zones [3]. This carrier displacement induces the presence of a space charge field that creates modifications of refractive indices via the electro-optic effect. For general considerations, another origin of the optical damage could be due to thermal effects, such as the thermo-optic effect that changes the refractive indices in the crystal due to a local heating induced by the power density of the laser beam. Nevertheless, in LN crystal, for relatively high power densities of the beam, these effects are negligible compare to the photorefractive effect [7]. It was proved that the optical damage threshold depends on the amount of intrinsic defects, and is considerably increased in stoichiometric LN and congruent LN doped with specific metal ions, such as Mg, Zn and in [8, 9]. Thus, to increase the optical damage threshold, two solutions exist. The first one consists of decreasing the number of intrinsic defects by growing LN crystals with the ratio $R = [\text{Li}]/[\text{Nb}]$ closer to the one corresponding to the stoichiometric composition (or close to it) but the growth of high quality crystals is difficult to obtain. The second approach consists in doping congruent lithium niobate crystals by appropriate doping ions because congruent crystals present a large amount of non-stoichiometric defects and, due to its complex defect structure, can accept a wide variety of dopants with various concentrations. Among possible dopant, we can site divalent ions such as Mg^{2+} [10, 11] and Zn^{2+} [12] or trivalent ions such as Sc^{3+} and In^{3+} , which are known, for specific concentrations, to improve the optical damage resistance of LN crystals. Recently, hafnium (Hf) was found to be a new optical damage-resistant element leading to a significant increase of the photorefractive resistance at doping threshold concentration around 2 mol% in the melt [13–18]. It has been found that the light-induced birefringence changes of LiNbO_3 crystal doped with 4 mol% of HfO_2 were comparable to that of 6 mol% MgO doped crystals. This concentration of hafnium correspond to the threshold concentration predicted by the charge compensation approach equal to the half of the Nb excess concentration between 3 and 4 mol% in a congruent crystal, i.e. $[\text{Hf}] = ([\text{Nb}] - [\text{Li}])/2$, with the notation $[\]$ corresponding to the mol% concentration of species. By else, the advantage of Hafnium is also a distribution coefficient near one at the threshold concentration so that high quality LN:Hf crystals may be easier to grow than the usual LN:Mg crystal with MgO 6% having a distribution coefficient closer than 1.2 [19]. Starting with these crystal physical properties and growth considerations, some crystal grower groups as the one of Kokanyan et al who proposed for the first time tetravalent impurity ions including Zirconium as new non-photorefractive ions [13, 20]. It was shown that zirconium presents a distribution coefficient closer to one for a zirconium threshold concentration in doped LN crystals latter found around 2.0 mol%. Even if all authors working in this research field suggest that Zr might represent an excellent alternative for obtaining higher optical damage resistance crystals with high optical quality, contradictory data concerning this threshold concentration are reported in literature [21–23]. It is therefore of interest for EO modulation or Q-switching applications, to know the EO coefficients values of zirconium- doped lithium niobate crystals as function of concentration over a wide frequency range from DC up to high frequencies.

This knowledge is so as important since, in addition to photoconductivity, photorefractive behavior is linked to the EO properties. It is reminded that the high-frequency or constant-strain (clamped) coefficient r^S is the true EO coefficient due to the direct modulation of the refractive indices by the applied electric field, in contrast to the low-frequency or constant-stress (unclamped) coefficient r^T , which includes in addition the contribution of the lattice deformation by the electric field. As a consequence we have carried out EO measurements over a wide frequency range and we report for the first time both clamped and unclamped EO coefficients values versus Zr concentration.

In the present contribution, we report, as function of zirconium concentration, experimental results and analysis obtained in the characterization of the EO coefficients r_{222}^T and r_{222}^S mainly involved in Q-switch laser applications. The coefficient r_{222} is obtained when a light-beam is propagating along the optical axis (c-axis) of the crystal and, therefore with an optical polarization of the transmitted beam in the isotropic plane, which renders it unaffected

by the temperature dependence of the birefringence within this configuration. The EO results would be then discussed based on the absorption spectrum of the grown crystals. To complete the study, we have measured the frequency dependence of the corresponding dielectric permittivity ϵ_{22} and finally established the figure of merit allowing the comparison between materials, used as modulator, dedicated for Q-switching applications.

2. Experimental

2.1 Sample preparation

Based on the Czochralski technique, a growth set-up using a single platinum crucible with rf heating element in air atmosphere was used to grow a set of Zr-doped lithium niobate crystals. In order to obtain directly during the growth process single-domain crystals, a dc electric current with a density of about 12 A/m^2 passed through the crystal-melt system. The starting materials used for sintering the lithium niobate charges of congruent composition were high purity Nb_2O_5 and LiCO_3 compounds from Johnson-Matthey and Merck. ZrO_2 was introduced into the melt with concentration equals to 0.625, 0.75, 0.875, 1.00, 1.25, 1.50, 2.00 and 2.50 mol%, respectively. Finally, samples were shaped in a parallelepiped shape with about $x, y, z = 5, 10, 5 \text{ mm}$ dimensions and were optically polished on all the surfaces.

The record of the UV-Visible-NIR optical transmission spectra reveals the optical qualification of the samples. Transmission spectra were recorded at room temperature with an un-polarized light using a Perkin Elmer Lambda 900 spectrometer. Samples were placed with their polished faces at normal incidence, with the c (z) axis parallel to the k vector of the incident light. The transmission spectra recorded in all crystals present same behaviors with a flat transparency response in the whole visible range and an absorption edge appearing in the UV. The fundamental absorption edges of the crystals were measured at the absorption coefficient of 20 cm^{-1} . Additionally to the good transparency without absorption parasitic peaks observed in all samples, these spectra bring interesting information on the role and influence of the dopant in lithium niobate crystals [24]. This point will be discussed further. However, we have plotted the interesting part for the present work of the absorption coefficient spectra and the absorption edges for the various samples, presented in Fig. 1. We observe a clear displacement of the absorption edge to UV when the concentration increase in the crystals up to 2 mol% of zirconium, whereas for crystal doped with higher concentration, the displacement of the absorption edge is to the visible wavelengths. The zirconium concentration of 2 mol% in congruent LN crystal, which corresponds to the minimum observed in the absorption edge position can be considered as a threshold concentration.

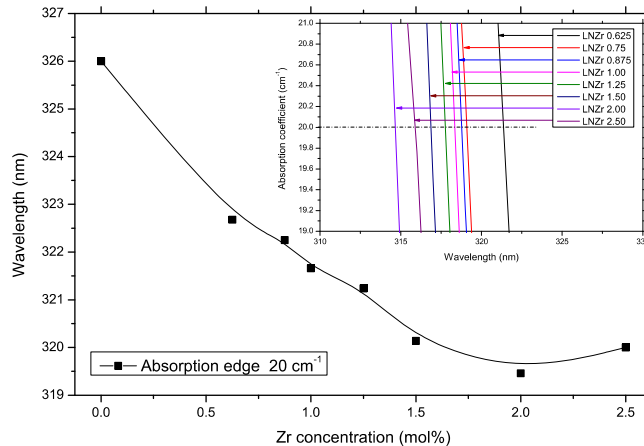


Fig. 1. Absorption edge versus Zr concentration in congruent LN doped crystals evaluated from absorption spectra. Insert: Zoom of the absorption spectra in the range of the absorption edge.

2.2 Electro-optic measurements

For EO measurements, we used an experimental setup based on the Sénarmont arrangement with the transfer function presented in Fig. 2.

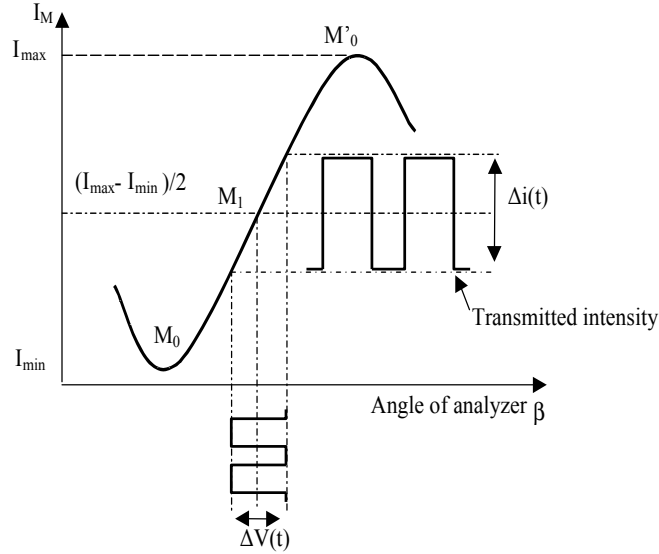


Fig. 2. Optical transmission function of Sénarmont setup versus the angle of the analyzer β and applied voltage. The point M_0 is the minimum transmission point for which the output optical signal has a frequency twice the frequency of the applied electric field. M_1 is the 50% transmission point yielding the linear replica of the ac voltage.

The point M_1 locates at 50% transmission $(I_{\max} - I_{\min})/2$ point corresponds to the so-called linear working point. It is associated with the “*Modulation Depth Method*” (MDM) [25] and can be used to determine the EO coefficient as a function of frequency from DC to 1 MHz defined by the specifications of power supply and signal acquisition electronic apparatus used for these experiments.

Measuring the peak-to-peak amplitude i_{pp} of the modulated signal at the point M_1 , one can obtain the EO coefficient directly from the following equation [25]:

$$r_{\text{eff}}(\nu) = \frac{2\lambda d}{\pi n_{\text{eff}}^3 I_0 L} \frac{i_{pp}(\nu)}{V_{pp}(\nu)} \quad (1)$$

Here, $I_0 = I_{\max} - I_{\min}$ represents the total intensity shift of the transfer function, L is the length of the crystal along the beam-propagation direction, d is the sample thickness along the applied electric field direction, n_{eff} is the effective refractive index, λ is the laser wavelength and V_{pp} is the peak-to-peak value of the applied ac field at the frequency ν .

The M_1 point can be also associated to a method called “*Time Response Method*” (TRM) [26]. At this working point, the instantaneous variation of the transmitted beam intensity $\Delta i(t)$ induced by the applied voltage $\Delta V(t)$ is given by:

$$\Delta i(t) = \frac{\pi n_{\text{eff}}^3 L I_0}{2\lambda d} r_{\text{eff}}(t) \otimes \Delta V(t) \quad (2)$$

where \otimes is the convolution operator and $r_{\text{eff}}(t)$ is the instantaneous value of the EO coefficient. As we can display and measure on an oscilloscope the time signals $\Delta i(t)$ and $\Delta V(t)$, the frequency dispersion of the EO coefficients can be derived from the ratio of $\Delta i(\nu)$ and $\Delta V(\nu)$ as obtained by the Z-transformation of the signals $\Delta i(t)$ and $\Delta V(t)$ respectively:

$$r_{eff}(\nu) = \frac{2\lambda D}{\pi n_{eff}^3 I_0 L} \frac{\Delta i(\nu)}{\Delta V(\nu)} \quad (3)$$

The optical response at short time leads to the clamped (high frequency) coefficient r^S , while the optical response at longer time provides the unclamped (low frequency) coefficient r^T .

We have shown that this technique allows obtaining the frequency dispersion of the EO coefficient from DC up to at least 500 MHz, mainly limited by the rising time of the voltage pulse [26]. It is to be mentioned that the values of the coefficients obtained by these techniques are absolute values.

For the specific experiments that are concerned by this work, electro-optic measurements were carried out by both MDM and TRM methods presented above. Within experiments devoted to the determination of the EO coefficient r_{222} the beam propagates along the c-axis of the sample and an external electric field was applied along the a-axis (or equivalently the b-axis).

The measurements were carried out at room temperature using a He-Ne laser ($\lambda = 633$ nm). In the MDM method, we used an ac voltage of 220 V peak-to-peak at 1kHz, whereas in the TRM method, a pulse of amplitude equal to 700V was applied onto the sample. Within these conditions, the sample dimensions and the performing optical and electric arrangements used for the experiment, the final uncertainty is in the order of 6% on the EO coefficients. By else, in the limit of the accuracy of the methods, no additional physical effects, as the distortion of the laser beam due to photorefractive effect or the presence of the quadratic electro-optic effect that could disturb the measurements were detected. Figure 3 shows the recording of both the applied voltage and the optical signal measured in the 0.8 mol%-Zr doped LN sample at different time within the TRM method. In the long-time range, the optical signal oscillates with periods corresponding to the main piezo-electric frequency resonances. In the short time, the two insets of Fig. 3 illustrate the EO response for different time scales. For time shorter than 350 ns the oscillations do not exist since the acoustic waves need more time to propagate across the crystal. The value of the intensity corresponding to the plateau appearing for time below 350 ns is much smaller than this obtained for time larger than 200 μ s, which indicates a large acoustic contribution (see Table 1).

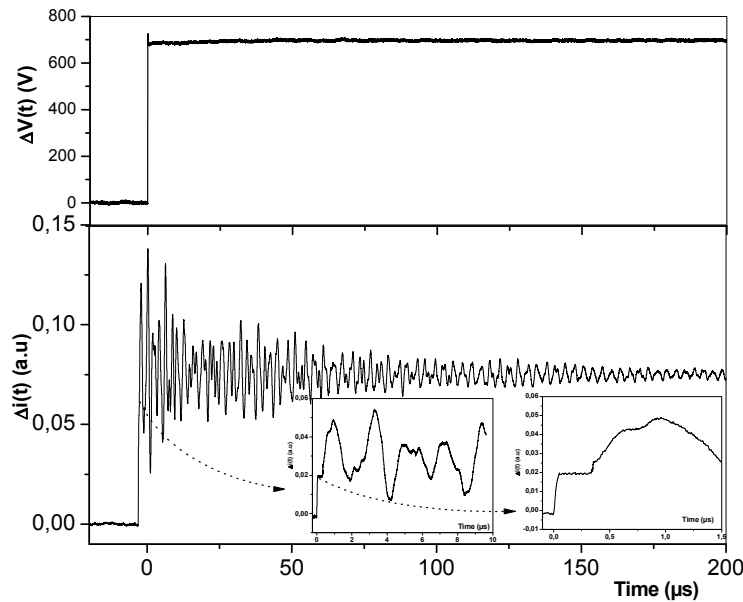


Fig. 3. Responses $\Delta i(t)$ to a step voltage $\Delta V(t)$ at different time scales in the case of the EO coefficient r_{222} in 0.8%-Zr doped LN single crystal. Measurements were performed at the wavelength of 633nm.

The frequency dispersion of the EO coefficient r_{222} is calculated according to Eq. (3). As shown in Fig. 4, the frequency dependence of the EO coefficient r_{222} of the crystal is flat on both sides of the piezo-resonances, giving, for this crystal doped with 0.8 mol% of zirconium the values of the EO coefficient at high frequency $r_{222}^S = 3.9 \pm 0.3$ pm/V and at low frequency $r_{222}^T = 6.6 \pm 0.4$ pm/V which are in a good agreement with those measured with the MDM method (see Table 1).

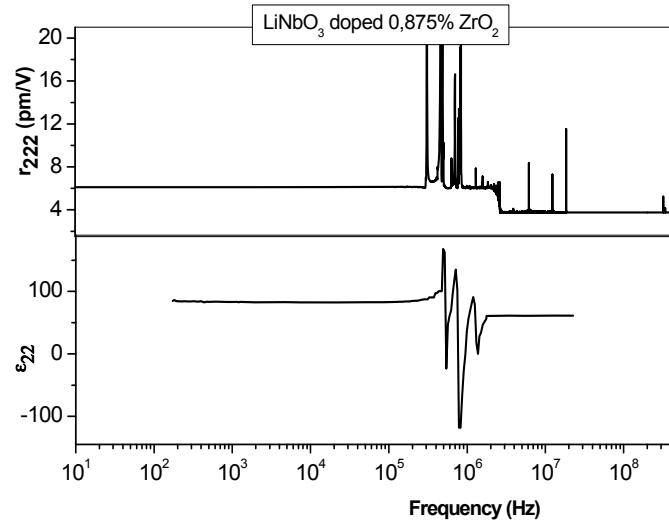


Fig. 4. Comparison of the frequency dispersions of the dielectric permittivity ϵ_{22} and of the EO coefficient r_{222} in the 0.8 mol% Zr-doped LN crystal.

The measurements of the coefficient r_{222} were performed for each crystal under investigation. All crystals present the same behavior as function of frequency. The dependence of the clamped and unclamped EO coefficients, r_{222}^T and r_{222}^S on the molar Zirconium concentration is shown in Fig. 5 and presented in Table 1.

We can see in Fig. 5 that both clamped and unclamped EO coefficients r_{222} present a kink around 2.0 mol% Zr. This kink in the EO properties of LN:Zr was already suggested in literature by Argiolas *et al* [23]. The values of the low- and high- frequency r_{222} coefficients in Zr-doped LN in the case of 2.0 mol% are equal to $r_{222}^T = 5 \pm 0.4$ pm/V and $r_{222}^S = 2.9 \pm 0.3$ pm/V, respectively corresponding to a decrease of about 25% of the values obtained in the other samples in the zirconium doped series. It is important to note that the observed kink has a value much greater than the uncertainty obtained in the measurements (equal to 6%).

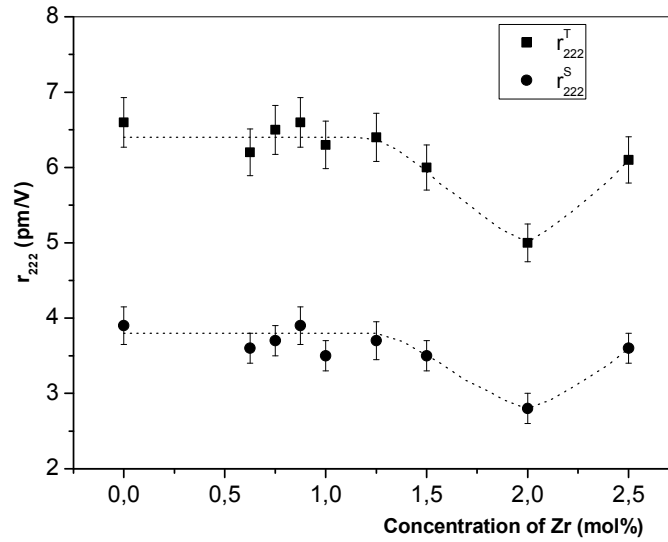


Fig. 5. EO coefficient r_{222}^T and r_{222}^S versus Zr concentration in congruent LN.

We note that contrary to Hf-doped LN crystals [16, 27], the value of r_{222} coefficient versus Zr concentration in LN:Zr crystals has to be emphasized since this coefficient presents a non-monotonous dependence as for crystals doped with other ions such as Zn or Mg [28, 29].

2.3 Dielectric measurements

In ferroelectric inorganic materials, it was established that the EO properties are linked to the linear dielectric properties. In particular, it was shown that the frequency dependence [30] of an EO coefficient reproduces the behavior of the corresponding dielectric permittivity ϵ . Such a link between ϵ and r still exists in their dependence on the dopant composition.

We have undertaken the measurements of the dielectric permittivity ϵ_{22} as function of frequency for all crystal-samples. Using a low voltage equal to 1V, inducing an electric field in sample under test equal to 1kV/m, the dielectric measurements were done by means of two impedance analyzers HP4151 and HP4191A in frequency ranges from 1 Hz to 13 MHz and from 1 MHz to 1GHz, respectively. The frequency dispersion of dielectric permittivity ϵ_{22} of the 0.8 mol%-Zr doped LN crystal measured along the c-axis is shown in Fig. 4. All samples present the same general response with the frequency being such that the Zr-concentration dependence of the clamped and unclamped permittivities ϵ_{22}^T and ϵ_{22}^S present a same kink-behavior as the EO coefficient r_{222} as shown in Fig. 6.

All data are reported in Table 1. As expected, the behavior of ϵ_{22} with frequency is very similar to this of r_{222} . In Fig. 4, we can see that ϵ_{22} displays a jump between both sides of the piezoelectric resonances, which corresponds to the electromechanical contribution $\Delta\epsilon$ to the static permittivity ϵ^T . This will be commented and discussed below.

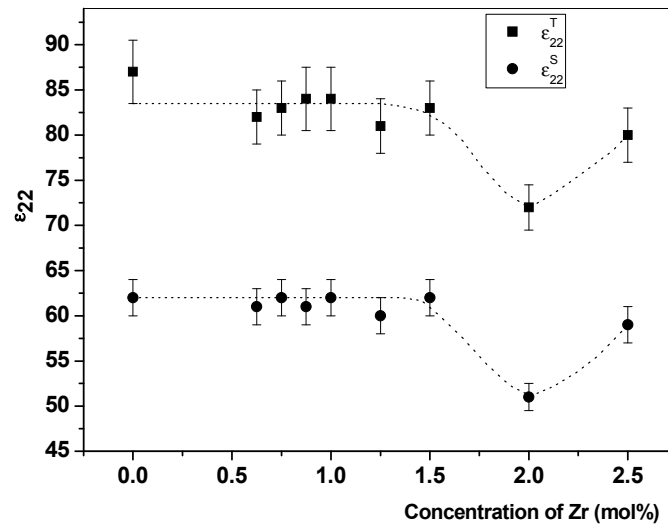


Fig. 6. Dielectric constant ϵ_{22}^T and ϵ_{22}^S versus Zr concentration in congruent LN.

Table 1. Absolute values of the r_{222} EO coefficient and related parameters of LN:Zr crystals as function of zirconium concentration: The EO coefficients at constant stress (r^T) were obtained by both MDM and TRM methods and at constant strain (r^S) by the TRM method, at 633 nm and at room temperature. The dielectric permittivities ϵ_{22}^T and ϵ_{22}^S were measured at room temperature. The figure of merit $F = n^7(r_{222}^S)^2/\epsilon_{22}^S$ was calculated from experimental values.

	MDM method	TRM method		Acoustic contribution	Dielectric constants		Figure of merit
	r_{222}^T (pm/V)	r_{222}^T (pm/V)	r_{222}^S (pm/V)	$r_{222}^T - r_{222}^S$ (pm/V)	ϵ_{22}^T	ϵ_{22}^S	$n^7(r_{222}^S)^2/\epsilon_{22}^S$ (pm/V) ²
LN-Cg	6,4 ± 0,4	6,6 ± 0,4	3,9 ± 0,3	2,7 ± 0,4	87 ± 5	62 ± 3	20
0,625%ZrO ₂	6,1 ± 0,4	6,1 ± 0,4	3,5 ± 0,3	2,6 ± 0,4	82 ± 5	61 ± 3	18
0,75%ZrO ₂	6,2 ± 0,4	6,5 ± 0,4	3,7 ± 0,3	2,8 ± 0,4	83 ± 5	62 ± 3	19
0,875%ZrO ₂	6,4 ± 0,4	6,6 ± 0,4	3,9 ± 0,3	2,7 ± 0,4	84 ± 5	61 ± 3	20
1%ZrO ₂	6 ± 0,4	6,2 ± 0,4	3,5 ± 0,3	2,7 ± 0,4	84 ± 5	62 ± 3	18
1,25%ZrO ₂	6,3 ± 0,4	6,4 ± 0,4	3,7 ± 0,3	2,7 ± 0,4	81 ± 5	60 ± 3	19
1,5%ZrO ₂	6,1 ± 0,4	6 ± 0,4	3,5 ± 0,3	2,5 ± 0,4	83 ± 5	62 ± 3	18
2%ZrO ₂	5,2 ± 0,4	5 ± 0,4	2,9 ± 0,3	2,1 ± 0,4	72 ± 4	51 ± 3	18
2,5%ZrO ₂	6 ± 0,4	6,1 ± 0,4	3,6 ± 0,3	2,5 ± 0,4	80 ± 5	59 ± 3	19

3. Discussion

We discuss the frequency and Zr concentration dependences of the EO coefficients. It is well known that the frequency dependence of the EO coefficients in crystals reflects the various physical processes contributing to the EO effect according to the working frequency [31]. In inorganic crystals the contribution arising from optical phonons is responsible for a large value at high frequency r^S . In piezo-electric crystals, the EO coefficient measured under low-frequency electric field or DC electric field arises from additional contribution related to the crystal deformation via the piezo-electric and the elasto-optic effects. This additional contribution is the so-called acoustic or piezo-optic contribution, denoted r^a and is therefore given by the difference between the unclamped r^T and clamped r^S coefficients. It can be thus derived from the experimental values of the EO coefficients measured below and above the piezo-electric resonances. We can observe a slight dependence of the acoustic contribution on Zr concentration, which is found $r_{222}^a = r_{222}^T - r_{222}^S = 2.1 \pm 0.4$ pm/V in the case of the 2.0% Zr-doped LN crystals.

By else, even if the dependence of all physical properties on zirconium concentration in lithium niobate is still not available, we are able to interpret rather trustfully our experimental results. The acousto-optic contribution to the electro-optic effect, r^a can be estimated from the elasto-optic (Pockels) p_{ijkl}^E at constant electric field, and from the piezoelectric d_{kij} tensors [32]

$$r_{ij,k}^a = \sum_{lm} p_{ij,lm}^E d_{lm,k} \quad (4)$$

Likewise, the difference between the low- and the high- frequency values of dielectric permittivity recorded on both sides of the acoustic resonances, $\Delta\epsilon_{ij}$ is expressed as:

$$\Delta\epsilon_{ij} = \epsilon_{ij}^T - \epsilon_{ij}^S = \sum_{kl} d_{ij,k} e_{kl} = \sum_{kl} d_{ij,k} C_{ijkl}^E d_{l,ij}, \quad (5)$$

where e is the piezoelectric stress tensor and C^E is the tensor of the elastic constants at constant electric field or elastic stiffness. Therefore the difference $\Delta\epsilon$ corresponds to the electromechanical contribution to the static permittivity ϵ^T .

It is to be noted that the coefficients $p_{ij,lm}^E$ can be also expressed with coefficients C_{ijkl}^E and e_{kl} using the thermodynamic relations. According to the point group 3m of LN crystal [32, 33], and by application of Neumann's principle to the p , d and C^E tensors followed by the use of the reduced-subscript notation, we obtain the piezo-optic contribution to r_{222} from Eq. (4)

$$r_{222}^a = -(p_{11}^E - p_{12}^E) d_{22} + p_{14}^E d_{15} \quad (6)$$

and the piezo-optic contribution to ϵ_{22} from Eq. (5) as

$$\Delta\epsilon_{22} = 2d_{22}^2 (C_{11}^E - C_{12}^E) - 4d_{22} d_{15} C_{14}^E + d_{15}^2 C_{44}^E, \quad (7)$$

Using the values of piezo-electric and elasto-optic coefficients, available in literature [34, 35] for the congruent composition only, we found (Eq. (6)) $r_{222}^a = 2.7 \text{ pmV}^{-1}$ in a good agreement with the experimental value, within the experimental error (10%) (see Table.1). This piezo-optic contribution is relatively large in LN since it constitutes nearly 40% of the total value $r_{222}^T \sim 6.6 \text{ pmV}^{-1}$.

Within Eq. (7), also evaluated for pure congruent lithium niobate, we found $\Delta\epsilon_{22} = 35$, which is close to the step directly detected in the experiments between both sides of the piezo-resonances.

We have demonstrated in our experiments that both the unclamped and clamped EO coefficients r_{222} and the dielectric permittivity ϵ_{22} present a kink at a threshold zirconium concentration of around 2 mol% and that the steps $\Delta\epsilon$ and r^a are only slightly changed when Zr is introduced in the LN lattice. From the above consideration, this large step between low- and high-frequencies in both the EO coefficient r_{222} and the dielectric permittivity ϵ_{22} in LN:Zr is mainly due to the large electromechanical process which constitutes the main contribution in the congruent material. We also note that the term included C_{44} is the largest in the congruent crystal even if it is too small to explain itself the piezo-optic contribution to ϵ_{22} .

Thus, the slight changes in the electro-optic coefficient and dielectric constant can be attributed to a slight changes in piezo-electric and elasto-optic coefficients in doped crystals and generally to the strain effects along a (or b) axis.

Now, considering the change in the electro-optic properties, appearing in the sample doped with 2 mol% of zirconium, we can note that this concentration corresponds to the threshold concentration determined in absorption measurements. However, Kovacs et al. have shown that the absorption edge is affected by the Li/Nb ratio [24]. Therefore, below the threshold concentration, the reduction in the absorption edge can be attributed to the increase

of the Li/Nb ratio due to the substitution by Zr ions of Nb ions on lithium site, i.e. on antisite Nb_{Li} . The increase of the absorption edge for higher concentration, above the threshold concentration, is linked to the disorder induced by zirconium incorporation on both Li and Nb sites and to the necessary charge compensation process. Thus, the threshold concentration can be explained by the existence of doping-induced lattice reorganization. The threshold observed in the EO and optical properties is in coincidence with the photorefractive concentration threshold observed by straightforward photorefractive measurements in Ref [27].

In addition, as concerns the applications of lithium niobate crystals, we have calculated the figure of merit linked to the driving voltage and the power (switching speed) of an EO modulator [36] or of a Pockels cell [37]. This figure of merit qualifies EO devices used as modulators or Q-switches and is defined as $F = n^7 (r_{222}^S)^2 / \epsilon_{22}$. The values of F obtained in the present study for the LN:Zr samples are listed in Table 1. We remark that F is quasi constant for all samples regardless the zirconium concentration even for the crystal at the threshold position. As, the figure of merit F , qualifying electro-optical devices, is preserved by Zr doping and due to its highly optical damage resistant, the crystal with 2.0 mol% concentration can be a promising material for EO modulation and Q-switching applications.

4. Conclusion

We have determined the unclamped and clamped values of the electro-optic coefficients r_{222} , and the corresponding dielectric permittivity ϵ_{22} as well, in Zr-doped LiNbO_3 crystals with varying Zr concentration. The frequency dependence of the EO coefficient reflects this of the associated permittivity. The piezo-optic contribution of the EO coefficient is much larger in r_{222} , which is mainly related to the stronger electric field induced –deformation along the a (b) axis, as reflected by the difference between the low-and high-frequency values of ϵ_{22} .

Both EO and dielectric coefficients reveal a small dependence on the Zr content introduced in the LN lattice and present a kink at 2.0 mol%, which is attributed to the strain contribution related to the introduction of Zr ions. Otherwise, if compared to undoped congruent crystal, the zirconium doped lithium niobate crystals present the advantage to have a smaller photorefractive damage, especially for concentration equal 2.0 mol%, and therefore should be more suitable for EO and NLO applications.